Aalborg Universitet

Single-pass hybrid laser welding of 25 mm thick steel

Farrokhi, Farhang; Larsen, Raino Mikael; Kristiansen, Morten

Published in:
Physics Procedia

DOI (link to publication from Publisher):
10.1016/j.phpro.2017.08.019

Creative Commons License
CC BY-NC-ND 4.0

Publication date:
2017

Document Version
Publisher's PDF, also known as Version of record

Link to publication from Aalborg University

Citation for published version (APA):
Farrokhi, F., Larsen, R. M., & Kristiansen, M. (2017). Single-pass hybrid laser welding of 25 mm thick steel. *Physics Procedia*, *89*, 49-57. https://doi.org/10.1016/j.phpro.2017.08.019

General rights
Copyright and moral rights for the publications made accessible in the public portal are retained by the authors and/or other copyright owners and it is a condition of accessing publications that users recognise and abide by the legal requirements associated with these rights.

- Users may download and print one copy of any publication from the public portal for the purpose of private study or research.
- You may not further distribute the material or use it for any profit-making activity or commercial gain
- You may freely distribute the URL identifying the publication in the public portal -

Take down policy
If you believe that this document breaches copyright please contact us at vbn@aub.aau.dk providing details, and we will remove access to the work immediately and investigate your claim.

Downloaded from vbn.aau.dk on: December 04, 2025

Available online at www.sciencedirect.com

ScienceDirect

Physics Procedia 89 (2017) 49 – 57

Physics Procedia

Nordic Laser Materials Processing Conference, NOLAMP_16, 22-24 August 2017, Aalborg University, Denmark

Single-pass hybrid laser welding of 25 mm thick steel

Farhang Farrokhi*, Raino Mikael Larsen, Morten Kristiansen

Aalborg University, Department of Materials and Production, Fibigerstraede 16, Aalborg 9220, Denmark

Abstract

The manufacturing of large steel structures involves welding thick-section steels. Using hybrid laser welding, it is possible to reduce production costs significantly. However, avoiding solidification cracks in the weld is difficult when welding thick-section steels. In this study, a number of experiments were performed on the hybrid laser welding of 25 mm steel. Different techniques of full penetration and partial penetration welding were discussed. Crack-free welds were obtained using single-pass or two-pass welding techniques. The results of the experiments showed that the joint preparation method and the penetration mode are very important factors in obtaining crack-free welds in welding thick section steels. With the same process parameters applied to hybrid laser welding, partial penetration welds were more susceptible to cracking than full penetration welds. This was partly attributed to a change in the melt flow and, consequently, a different solidification mode that occurred during the full penetration mode welding.

© 2017 The Authors. Published by Elsevier B.V. This is an open access article under the CC BY-NC-ND license (http://creativecommons.org/licenses/by-nc-nd/4.0/).
Peer-review under responsibility of the scientific committee of the Nordic Laser Materials Processing Conference 2017

Keywords: Hybrid laser welding; solidification mode; solidification cracking; joint preparation; thick-section steel.

1. Introduction

With ongoing technical development and the increasing power levels of high power solid-state lasers, heavy industries such as shipbuilding, offshore windmills, power plants, and pipelines industries are looking for new opportunities to substitute their conventional welding methods with hybrid laser welding (Nielsen 2015). Hybrid laser-GMA welding is a promising welding process and is capable of processing thick-section steels as it can compensate for the limitations in laser welding and Gas Metal Arc (GMA) welding by utilizing the features of both.

* Corresponding author.
E-mail address: ffk@m-tech.aau.dk

1875-3892 © 2017 The Authors. Published by Elsevier B.V. This is an open access article under the CC BY-NC-ND license (http://creativecommons.org/licenses/by-nc-nd/4.0/).
Peer-review under responsibility of the scientific committee of the Nordic Laser Materials Processing Conference 2017
doi:10.1016/j.phpro.2017.08.019

Despite the advantages of this process, the control of solidification cracks is still a key challenge when it comes to welding thick-section steels. In general, solidification cracking appears on the weld centerline and occurs in the fusion zone in the final stage of solidification, when a liquid film may appear along the solidification boundaries. It is, in fact, the inability of this liquid film to deal with shrinkage-induced strain and extrinsic mechanical strain during solidification and subsequent cooling of the weld that results in the formation of a solidification crack (Lippold 2015). The cause of hot cracking can ultimately be attributed to the complex interaction between the main influences of welding parameters, the chemical composition of the alloy, and restraint intensity (Cross 2005). One of the crucial ways to control restraint intensity, which is one of the main interests of this paper, is the design of joint geometry and welding sequences. With the optimum design, it is possible to control not only mechanically induced strains but also thermally induced strains by controlling cooling rate and heat dissipation through the component.

The manufacture of large structures often involves welding steel plates with thicknesses of 20 mm or more. However, when experimental research investigated the design of joint geometry and welding sequences and the chance of cracking on the hybrid solid-state laser welding of structural steels, only a few investigations used wall thicknesses exceeding 20 mm. For example, Vollersten et al. (2010) and Rethmeier et al. (2009) conducted studies on welding X65 pipe steel up to 20 and 32 mm thick, respectively, and suggested using either a beveled groove (Y-groove) or preheating to obtain sound joints. They performed a one-sided multi-pass welding procedure in which hybrid laser welding was used only for the root pass. Gook et al. (2014) suggested a double-sided welding procedure for 23 mm X80 pipe steel, but they used hybrid laser welding only for the root pass of Y-grooves where the root welding was performed from the flat side. Wahba et al. (2016) developed a new single-pass hybrid laser welding technique on 25 mm SM490A low-alloyed steel. They used a 2.5 mm gap in butt joint configuration, filled up with cut wires and supported by backing. All these experiments that yielded crack-free welds used hybrid laser welding only for one pass where full penetration of the sample thickness was achieved and where there was no solid material below the bottom of the laser weld. However, when hybrid laser welding was used for double-sided partial penetration welding of 20 and 25 mm thick steel in Akselsen et al. (2013) and Farrokhi et al (2015, 2016), solidification cracks could not be avoided in the welds. This leads to the assumption that a correlation exists between the chance of solidification cracking and the *penetration mode* (full/partial) of hybrid laser welding.

Two mechanisms related to the difference between full and partial penetration laser welding could explain this phenomenon: (i) melt flow dynamics (Schaefer et al. 2015), and (ii) thermal and mechanical induced stresses (Gebhardt 2013). Schaefer et al. (2015) analyzed the influence of laser beam quality and parameters on the formation of solidification cracks in tempered steels. They observed that crack formation could be avoided when full penetration of the sample thickness was achieved, while partial penetration experiments required cautious optimization of beam parameters to avoid solidification cracks. In a recent study, Schaefer et al. (2017) also related the formation of cracks to melt flow dynamics, which, according to their previous study, differ in full and partial penetration laser welding (Schaefer et al. 2015). Moreover, Gebhardt et al. (2012) conducted an experimental study on the full and partial penetration hybrid laser welding of a number of different carbon steels with wall thicknesses up to about 15mm. They reported that crack-free welds were obtained only when full penetration welding was carried out and shrinkage restraint was limited. This was later confirmed by a numerical analysis carried out on S460NH low-alloyed high strength steel (Gebhardt 2013). The results showed that higher magnitude of stresses occurred in the partial penetration mode and in the regions that solidification cracks were found in the experiments.

The above review shows that despite the importance of the subject, only a limited number of studies have related the effect of penetration mode and the design of weld sequences to the chance of cracking. Moreover, preparation methods other than milling, such as laser cutting, have not been taken into account. Accordingly, this paper aims to provide more experimental data on the qualitative and microstructural differences between full and partial penetration in hybrid laser welding. In addition, two welding procedures with novel preparation methods were introduced for the single-pass and two-pass welding of 25 mm thick steel. Both procedures used full penetration and single-pass hybrid laser welding technique to reduce the chance of cracking.

2. Experimental procedure

Steel plate of type S355J2 was used for the experiments. The chemical composition of the steel can be found in Table 1. Plates with dimensions of 25 x 60 x 120 mm were used to form 25 x 120 x 120 butt joints. Steel plates with such thicknesses of up to 25 mm are often used for the manufacture of large and heavy structures, limiting the gap variation during welding. Therefore, to allow more realistic experiments, two blocks of the same material were tack welded to both sides of the samples to limit the gap variation. This also made it possible to keep the start and stop points outside the main plate. Two techniques of joint preparation were used for the one-sided welding of 25 mm steel, which is described in the following two sub-sections.

The laser used for welding was a Trumpf TruDisk 16002 disk laser providing a 16 kW continuous-wave laser beam with a wavelength of 1030 nm. The laser was guided through an optical fiber to a Trumpf RFO with a focal length of 600 mm. The hybrid laser welding combined the laser and a MAG system with a gas containing 92%Ar and 8%CO_2. The filler material was ESAB OK 12.50 filler wire with a diameter of 1.2 mm. After welding, radiographic examination was performed to detect possible cracks in the welds. The weld samples were exposed to 210 kV x-ray radiation, giving an Image Quality Indicator (IQI) sensitivity of 1.6%. Macro-section samples were cut from each weld according to the crack indication locations (if any) on the digital radiographic images. Quality evaluation was restricted to a 70 mm long section in the middle of the weld. An optical microscope, equipped with an automatic image-stitching program, was used for microanalysis after the samples were etched with 2% Nital. Following the microanalysis, the samples were over etched using either 4% Nital or Ammonium peroxodisulfate etchants to obtain a better contrast for the macrographs imaging.

2.1. Single-pass welding procedure

The first joint preparation technique employs a *high-speed* laser cutting method, subsequently allowing a single-pass welding process. Accordingly, steel plates were first cut using a 3kW IPG YLS-3000SM single-mode fiber laser. The laser was guided through an optical fiber to a HighYag cutting head. The setup for cutting is illustrated in Kristiansen et al. (2013), and the cutting parameters can be found in Table 2. The high-speed laser cut surfaces formed a special *tulip-shaped* groove in the butt joint. As can be seen in Figure 1a, a 6 to 8 mm long root face was formed in the groove. However, the dimensions of the groove varied slightly in different sections of the specimens, even though the cut kurf shape remained more or less the same. To remove oxide layers, the cut surfaces were sand-blasted before welding. The welding was performed using an arc-leading process, while ceramic backing strips supported the joints at the root side. Figure 1b shows an overview of the experimental setup, and the welding process parameters can be found in Table 3.

Table 1. Chemical composition of the steel (%) (according to the material certificate provided by the steel manufacture).

	C	Mn	P	S	Si	Cu	Al	Ni	Cr	V	Mo	CEV
S355J2	0.15	1.44	0.013	0.006	0.22	0.08	0.035	0.04	0.06	0.002	0.007	0.41

Table 2. Laser cutting process parameters.

	Travel speed (mm/min)	Gas type	Gas pressure (bar)	Nozzle standoff (mm)	Nozzle diam. (mm)	Laser power (kW)	Focal length (mm)	Focal position (mm)
Hi-speed	675	O_2	1.1	0.9	2.5	3	470	35*
Low-speed	50	N_2	7.5	0.9	2.5	3	470	-12.5**

Notes: * Above the workpiece surface. ** Below the workpiece surface.

Table 3. Single-pass welding process parameters.

Laser power (kW)	Arc current (A)	Arc voltage (V)	Wire feed (m/min)	Travel speed (mm/min)	Gas flow rate (l/min)	Focal position (mm)	Laser angle (degree)	Arc torch angle (degree)	Wire stickout (mm)	Arc-laser distance (mm)
14	475	25	20	500	25	20*	-7**	20**	25	3

Notes: * Above the workpiece surface. ** With respect to the vertical axis.

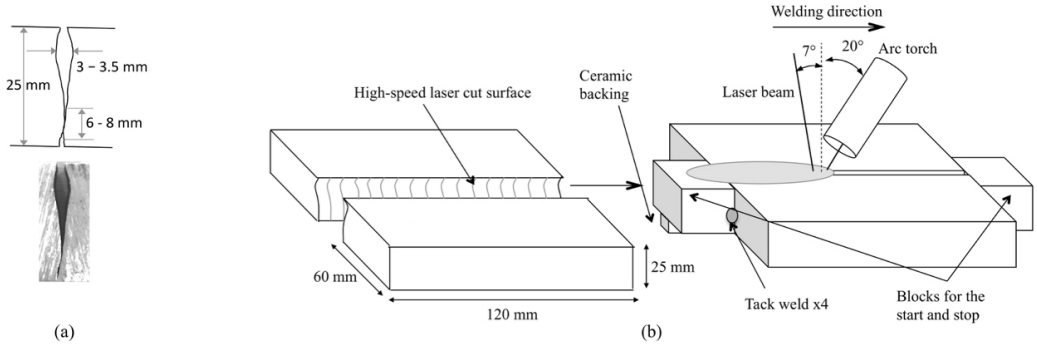

Fig. 1. Preparation and setup for single-pass welding: (a) groove geometry, (b) overall procedure.

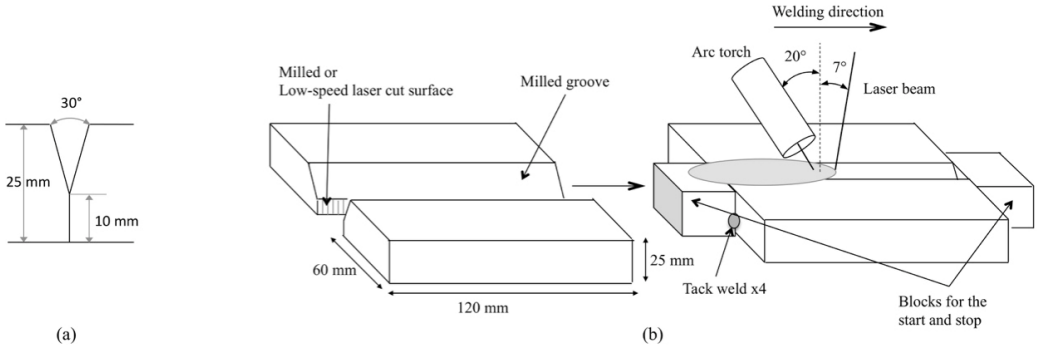

Fig. 2. Preparation and setup for Two-pass welding: (a) groove geometry, (b) overall procedure.

Table 4. Two-pass welding process parameters.

Laser power (kW)	Arc current (A)	Arc voltage (V)	Wire feed (m/min)	Travel speed (mm/min)	Gas flow rate (l/min)	Focal position (mm)	Laser angle (degree)	Arc torch angle (degree)	Wire stickout (mm)	Arc-laser distance (mm)
16	84	16	2	900	25	25*	-7**	20**	15	15
-	500	32	22	400	25	-	-	20**	15	-

Notes: * Above the workpiece surface. ** With respect to the vertical axis.

2.2. Two-pass welding procedure

The second joint preparation technique used a conventional machining/beveling method allowing a subsequent two-pass welding process in which a single-pass hybrid laser welding was used only for the root pass. Figure 2a shows the Y-groove that was used for this technique. The root welding was performed using a laser-leading configuration. Figure 2b shows an overview of the experimental setup, and the welding process parameters can be found in Table 4. To allow comparison, some samples were prepared using *low-speed* laser cutting and later beveled using milling. This meant that the root face of the Y-joints had a rough surface resulting from striations produced during the low-speed laser cutting process, an effect anticipated by Farrokhi and Kristiansen (2016). The low-speed laser cutting process parameters are presented in Table 2. The milled surfaces were cleaned using alcohol to remove the coolant liquid from the machining process. The lasers cut surfaces were sand-blasted to remove the oxide layer due to the laser cutting.

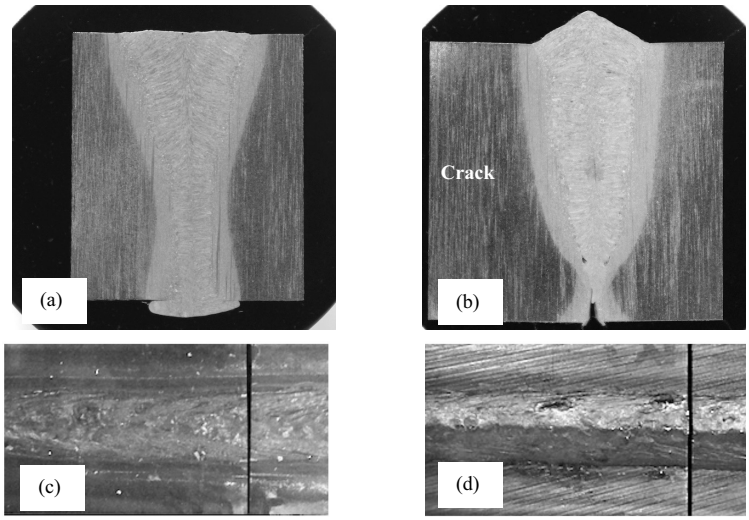

Fig. 3. Macro-section of single-pass welds: (a) full penetration experiment, and (b) partial penetration experiment with a crack in the center. Top view of the weld beads: (c) full penetration experiment, and (d) partial penetration experiment.

3. Results and discussion

3.1. Single-pass welding

The main challenge faced in single-pass welding was to avoid the melt pool dropping through the joint. This is why the backing was required during welding. However, as the root face length of the joints was about 6 to 8 mm (Figure 1a), careful control of laser power intensity was still required to avoid the melt pool dropping through the joint. On the one hand, the gravitational force due to the weight of the molten material together with the presence of excessive laser power could increase the chance of it dropping through. On the other hand, lowering the laser power would impede full penetration because a large amount of filler material was required to fill the entire groove in one pass, and this would absorb a large portion of the laser power. Therefore, the focal point position was set to 25 mm above the plate and welding with a defocused beam was used at the same laser power. In addition, an arc-leading configuration was chosen with the arc exposed one second before the laser was turned on.

3.1.1. Weld quality

Figure 3a shows an example of the macro-section of the single-pass welds. As can be seen in the figure, full penetration was achieved and crack-free joints were obtained. Three experiments were repeated for the same parameter set, and, according to the radiographic examination and the macro-section cuts, none of them contained cracks. As anticipated by Wahba et al. (2015), cold lapping occurred at the root side due to the low temperature melt flow in the vicinity of the curved-shape ceramic backing. However, alternative-backing materials such as submerged arc welding flux and fiberglass strips resulted in either drop through or lack of penetration. The results of single-pass welding using high-speed laser cutting as a preparation method indicate the great potential and importance of alternative joint preparation methods. Crack-free welds and a penetration depth of 25 mm were obtained using only 14 kW laser power. However, as the groove shape dimensions tended to vary slightly from sample to sample (Figure 1a), the process was not completely reproducible, and partial penetration occurred in some experiments. Interestingly, cracks appeared in partial penetration welds even though the process parameters and welding heat input were the same as for the full penetration experiments (Figure 3a and b). This leads to the assumption that cracks are more likely to occur in partial penetration welding, which is in conformity with the results of hybrid laser welding reported in Gebhardt et al. (2012, 2013) and laser welding reported in Schaefer et al. (2015). As the process parameters were the same for both

experiments, the filler material that could not completely penetrate during the partial penetration weld formed weld bead reinforcement on the face side (Figures 3c and d).

Further optimization of process parameters is required to enhance process repeatability. For example, it would be interesting to modify the tulip-shape laser cut surface (Figure 1a) by further optimization of the laser cutting process parameters. Alternatively, standard milled groove geometry could be adapted from the tulip-shape laser cut geometry to assure process reproducibility.

3.1.2. Microstructural analysis

Figure 4 shows the microstructure of the weld centerline in the crack-susceptible regions. In the case of full penetration welds (Figure 4a), the microstructure consisted of acicular ferrite and bainite, and the solidification mode in some cases seemed to be equiaxed dendritic. Similarly, the microstructure of partial penetration welds (Figure 4b) also consisted of acicular ferrite and bainite, but in this case the solidification mode was cellular or dendritic (epitaxial). The crack occurred when columnar growth was perpendicular to the weld centerline axis. This led to the assumption that partial penetration resulted in a columnar solidification mode, which increased the chance of cracking in the weld centerline.

Apart from thermal conditions in the weld centerline potentially favoring an equiaxed grain structure in full penetration welds, equiaxed grains will only form in the weld pool if nucleants such as dendrite sidearm or grain detachment are available or, alternatively, if nucleants are deliberately added, for instance by filler wire (Norman et al. 1998). In this study, the latter possibility could be discounted as the filler material used was the same for all the experiments. However, as with solidification mechanisms in ingots and castings, equiaxed structures may occur as a result of dendrite sidearm detachment induced by convection currents in the melt (Porter et al. 2009). This has also been reported by Norman et al. (1998) in a study of the laser welding of aluminum alloys. The implication for our study is that a favorable convection current may have occurred during the full penetration welding, leading to the formation of equiaxed structure in the weld centerline. Accordingly, it was possible to confirm the findings of Schaefer et al. (2015, 2017) that the formation of cracks could be related to melt flow dynamics, which differed in full and partial penetration laser welding. It is worth pointing out that the different convection currents of the experiments could also affect the thermal gradients and consequently the thermally induced stresses in the weld, which, to some degree, could influence the chance of cracking. Moreover, the influence of backing must be investigated as it could also affect the convection current and heat distribution in the weld.

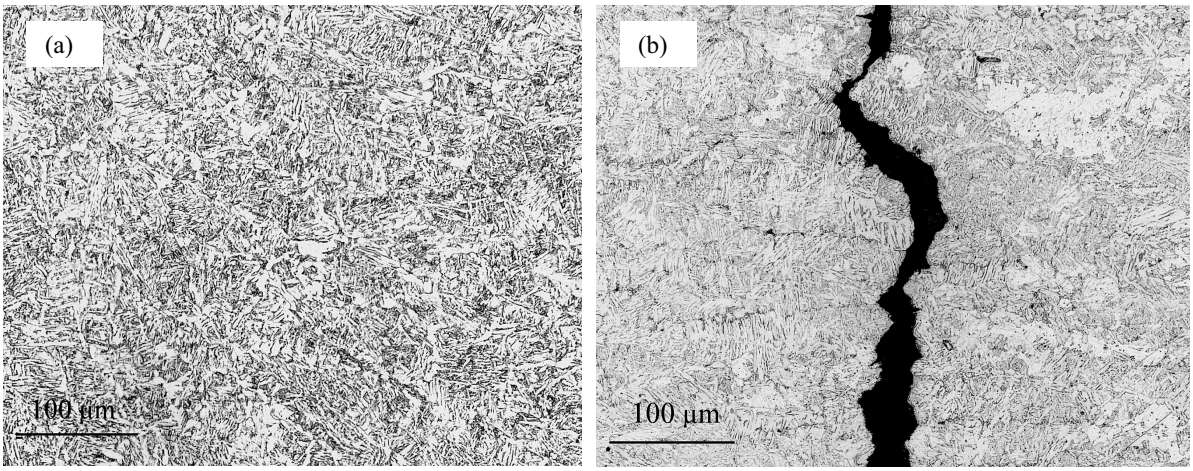

Fig. 4. Microstructure of the single-pass weld centerline in the crack-susceptible region: (a) full penetration weld, and (b) partial penetration weld that was cracked.

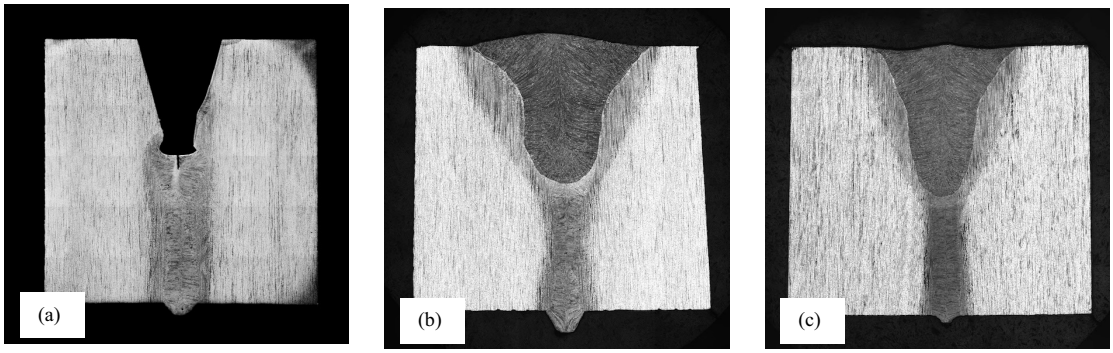

Fig. 5. (a) The root pass, (b) the complete two-pass weld, and (c) the modified weld using low-speed laser cutting as preparation method.

3.2. Two-pass welding

Y-joint configuration was used for this technique, in which first the root pass was performed using hybrid laser welding and the groove subsequently filled up only by GMA welding as the second pass. As the process parameters must be adapted to a given specific joint geometry, a different technique was used for the two-pass welding of Y-grooves. For this reason, the welding technique was changed to a laser-leading process with a defocused laser beam and minimal arc power (Table 4) to avoid the molten material dropping through the joint. Therefore, the hybrid laser welding for the root pass was rather similar to autogenous laser welding, and the arc power was meant to balance the heat input. The process did not require the use of backing because the heat input was relatively low during the root welding.

3.2.1. Weld quality

Figure 5 shows the macrograph of the welds. As can be seen in Figure 5a, a shallow and continuous solidification crack appeared in some cases on the weld bead surface of the root welds. However, the crack could be re-melted and healed during the second pass. Figure 5b shows an example of the complete two-pass weld macrograph. The macrographs and x-ray tests revealed no cracks in the welds of three replicates, and the experiments were 100% repeatable. However, the angle of the weld bead at the root side was too sharp in some cases. Optimization of the root shape using different welding speed was not possible. For instance, a 20% reduction of welding speed led to a wider root weld but did not reduce the root bead sharpness. Similarly, increasing the welding speed by up to 20% either resulted in extremely unsteady root humping or incomplete penetration. However, as Farrokhi and Kristiansen (2016) have suggested, the samples whose root faces were prepared by low-speed laser cutting yielded better results. This can be seen in Figure 5c. When low-speed laser cutting was used as joint preparation, not only could welding speed be increased, but also a very smooth and steady root weld could be obtained. The modified experiment shown in Figure 5c used the same welding parameters, except for the welding speed, which was 300 mm/min faster than the other experiments owing to the low-speed laser cutting method adopted for preparation.

3.2.2. Microstructural analysis

According to the microanalysis of the two-pass welding results, the second pass GMA weld microstructure consisted of acicular ferrite as well as proeutectoid ferrite (Figure 6a). As was expected, the root weld, which had the characteristics of autogenous laser welds, mainly exhibited bainitic microstructure with the columns bending towards the weld centerline axis (Figure 6b and c). Notably, despite the columnar solidification mode, the typical solidification

cracks, which usually appear in the mid-section of the laser welds, were absent in the root weld. This was attributed to the assumption that the stresses in the mid-section of the root weld were minimized due to the full penetration welding mode. Table 5 summarizes the results of the experiments discussed in this section.

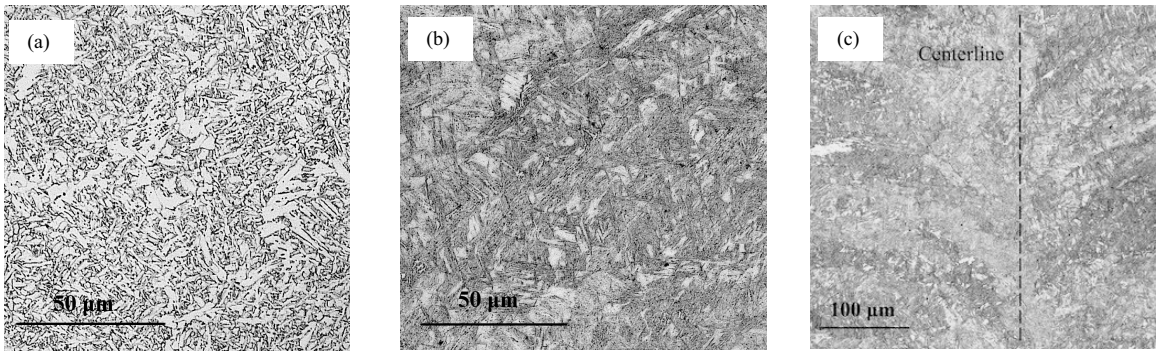

Fig. 6. Microstructure of the weld centerline: (a) the second pass weld, (b) the hybrid laser root weld with 50x, and (c) 20x magnification.

Table 5. Summary of the results and quality evaluation.

	* Penetration mode	No. of replicates	Line energy (kJ/mm)	Groove shape	Preparation	Solidification cracking	Reference
Single-pass welding	Full	3	3.1	Tulip-shape	Hi-speed laser cut	No	Fig. 3a
Single-pass welding	Partial	3	3.1	Tulip-shape	Hi-speed laser cut	Yes	Fig. 3b
Two-pass welding	Full (root)	3	1.1 (root)	Y-groove	**Low-speed laser cut	Healed	Fig. 5b, c

Notes: * penetration mode of the hybrid laser welding. **and/or milled.

4. Conclusion

In this study, two welding procedures were introduced for the single-pass and two-pass welding of 25 mm thick steel. The quality and microstructural properties of the welds were discussed with respect to the preparation method and the *penetration mode* of hybrid laser welding. On the basis of the results of the experiments, the following conclusions can be drawn:

- For the same process parameters, partial penetration welds were more susceptible to cracking than full penetration welds. This implies that hybrid laser welding sequences and groove geometry design have a crucial impact on weld solidification cracking.
- When using single-pass welding, partial penetration resulted in a columnar solidification mode, increasing the chance of cracking in the weld centerline. In the case of full penetration welds, however, the solidification mode in the weld centerline seemed to be equiaxed dendritic, which was attributed to a favorable convection current that occurred during welding. This implies that a correlation exists between melt pool dynamics and the occurrence of solidification cracking. Moreover, the influence of backing must be investigated as it could also affect the convection current and heat distribution in the weld.
- Crack-free welds could be obtained using single-pass and two-pass welding techniques. Both techniques were designed so that full penetration of the sample thickness was reached during the hybrid laser welding pass, and where there was no solid material below the bottom of the hybrid laser weld.
- Laser cutting could be adapted to prepare the subsequent hybrid laser welding process. Higher quality and faster root welds could be obtained with a *low-speed* laser cutting method than when milling was used for preparation. The use of a *high-speed* laser cutting method enabled a special groove shape to be obtained that made it possible to perform the single-pass welding of 25 mm thick steel using only 14 kW laser power.

Acknowledgements

This study was supported in part by the Danish National Advanced Technology Foundation project *Cost-Effective Mass Production of Universal Foundations for Large Offshore Wind Parks*. In addition, the authors would like to thank Force Technology for providing welding and radiographic examination facilities.

References

Akselsen, O. M., Wiklund, G., Østby, E., Sörgjärd, A., Kaplan, A., 2013. A first assessment of laser hybrid welding of 420 mpa steel for offshore structure application. In Proceedings of the 14th Nordic Laser Materials Processing Conference Nolamp 14, Luleå tekniska universitet.

Cross, C.E., 2005. On the origin of weld solidification cracking. In *"Hot cracking phenomena in welds"*, Springer Berlin Heidelberg, pp. 3-18.

Farrokhi, F., Nielsen, S.E., Schmidt, R.H., Pedersen, S.S., Kristiansen, M., 2015. Effect of Cut Quality on Hybrid Laser Arc Welding of Thick Section Steels. Physics Procedia 78, pp. 65-73.

Farrokhi, F., Kristiansen, M., 2016. A Practical approach for increasing penetration in hybrid laser-arc welding of steel. Physics Procedia 83, pp. 577-586.

Gebhardt, M. O., Gumenyuk, A., Quiroz Penaranda, V., Rethmeier, M., 2012. Laser/GMA hybrid welding of thick-walled precision pipes. Welding and cutting, 5, pp. 312-318.

Gebhardt, M. O., Gumenyuk, A., Rethmeier, M., 2013. Numerical analysis of hot cracking in laser-hybrid welded tubes. Advances in Materials Science and Engineering, 2013.

Gook, S., Gumenyuk, A., Rethmeier, M., 2014. Hybrid laser arc welding of X80 and X120 steel grade. Science and Technology of Welding and Joining, 19 (1), pp. 15-24.

Kristiansen, M., Selchau, J., Olsen, F.O., Hansen, K.S., 2013. Quality and performance of laser cutting with a high power SM fiber laser. In Proceedings of the 14th Nordic Laser Materials Processing Conference Nolamp 14. Luleå tekniska universitet.

Lippold, J.C., 2015. Welding Metallurgy and Weldability. John Wiley & Sons, Inc., New Jersey, pp 86.

Nielsen, S. E., 2015. High power laser hybrid welding–challenges and perspectives. Physics Procedia, 78, pp. 24-34.

Norman, A. F., Ducharme, R., Mackwood, A., Kapadia, P., Prangnell, P. B., 1998. Application of thermal modelling to laser beam welding of aluminium alloys. Science and Technology of Welding and Joining, 3(5), pp. 260-266.

Porter, D. A., Easterling, K. E., Sherif, M. 2009. Phase Transformations in Metals and Alloys, (Revised Reprint). CRC press, Boca Raton, pp. 233.

Rethmeier, M., Gook, S., Lammers, M., Gumenyuk, A., 2009. Laser-Hybrid Welding of Thick Plates up to 32 mm Using a 20 kW Fibre Laser. Quarterly journal of the Japan welding society, 27, pp. 74-79.

Schaefer, M., Speker, N., Weber, R., Harrer, T., Graf, T., 2015. Analysing hot crack formation in laser welding of tempered steel. In Proceeding of Lasers in Manufacturing Conference, LIM 2015. WLT.

Schaefer, M., Kessler, S., Scheible, P., Speker, N., Harrer, T., 2017. Hot cracking during laser welding of steel: influence of the welding parameters and prevention of cracks. In Proceedings of SPIE LASE. International Society for Optics and Photonics. pp. 100970E-100970E.

Vollertsen, F., Grunenwald, S., Rethmeier, M., Gumenyuk, A., Reisgen, U., Olschok, S., 2010. Welding Thick Steel Plates With Fibre Lasers and GMAW. Welding in the World 54, pp. R62-70.

Wahba, M., Mizutani, M., Katayama, S., 2016. Single pass hybrid laser-arc welding of 25mm thick square groove butt joints. Materials & Design, 97, pp. 1-6.